

# Frequency filtered storage of parametric fluorescence with electromagnetically induced transparency

K. Akiba<sup>1</sup>, K. Kashiwagi<sup>1</sup>, T. Yonehara<sup>1</sup>, and M. Kozuma<sup>1,2</sup>

<sup>1</sup>Department of Physics, Tokyo Institute of Technology,  
2-12-1 O-okayama, Meguro-ku, Tokyo 152-8550, Japan

<sup>2</sup>PRESTO, CREST, Japan Science and Technology Agency, 1-9-9 Yaesu, Chuo-ku, Tokyo 103-0028, Japan

(Dated: February 9, 2020)

The broadband parametric fluorescence pulse (probe light) with center frequency resonant on  $^{87}\text{Rb } D_1$  line was injected into a cold atomic ensemble with coherent light (control light). Due to the low gain in the parametric down conversion process, the probe light was in a highly bunched photon-pair state. By switching off the control light, the probe light within the electromagnetically induced transparency window was mapped on the atoms. When the control light was switched on, the probe light was retrieved and frequency filtered storage was confirmed from the superbunching effect and an increase of the coherence time of the retrieved light.

PACS numbers: 42.50.Gy, 42.50.-p, 32.80.Qk

Dark state polariton theory [1, 2] of electromagnetically induced transparency (EIT) [3] presents the possibility of coherently transferring a quantum state of light to an atomic collective excitation by manipulating control light, where the control light turns an opaque medium for a weak probe light into a transparent one. Such a quantum state transfer has been successfully demonstrated for nonclassical light generated from an atomic ensemble [4, 5, 6]. The advantage of generating nonclassical light from the atoms is that the bandwidth of the light is matched by the narrow atomic resonant width. Compared to the process of generating nonclassical lights with atoms, the parametric down conversion (PDC) process has been widely used in fundamental experiments in quantum optics [7, 8, 9] and for demonstrating various quantum information protocols [10, 11]. The process also enables the generation of rich nonclassical photonic states such as the antibunched state [12, 13], hyperentangled state [14] GHZ state [15], *W* state [16], and cluster state [17]. Storing such nonclassical light in atomic ensembles generates corresponding nonclassical atomic states. Furthermore, the state of the nonclassical light can be manipulated by applying an additional field to the atoms storing the photonic state or by changing the properties of the control light [18, 19, 20].

In this paper, we report frequency filtered storage of parametric fluorescence (highly bunched photon-pair state) with EIT. The frequency bandwidth of parametric fluorescence is typically of the order of  $10^{13}$  Hz, which is much broader than an atomic resonance interaction width ( $\sim 10^6$  Hz). The discrepancy between the frequency bandwidth and the resonance width presents a problem for photon counting in experiments, since photons interacting with atoms cannot be selectively counted. We avoided this problem in our experiments by utilizing the properties of the optical pulse propagation inside the EIT medium [1, 2, 21]. When the pulse spectrum was broader than the transparency window, the pulse was split into an adiabatic part having a spectrum within the transparency window and an oscillating non-

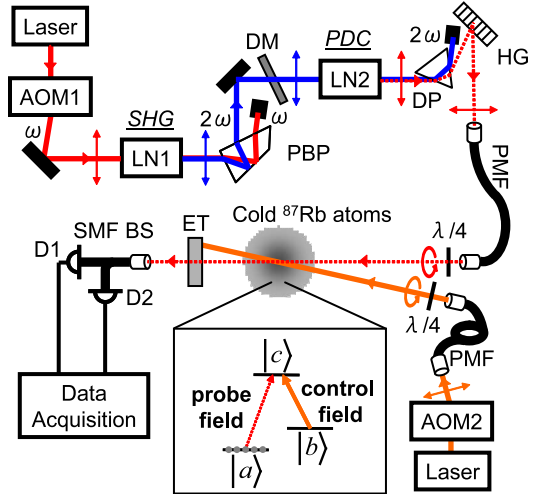


FIG. 1: (Color online) Schematic diagram of experimental setup. AOM: acousto-optic modulator; LN: quasi-phase-matched  $\text{MgO:LiNbO}_3$  waveguide; PBP: Pellin Broca prism; DM: dichroic mirror; DP: dispersing prism; HG: holographic grating; PMF: polarization maintained single mode fiber;  $\lambda/4$ : quarter wave plate; ET: etalon; BS: beam splitter; SMF: single mode fiber; D1, D2: avalanche photodetectors.

adiabatic part. The control light was turned off when the pulse was propagating in the medium, thus storing the adiabatic part. After the nonadiabatic part passed through the medium, the control light was turned on, allowing the retrieved adiabatic part to be separated from the nonadiabatic part in time. We call this technique as time-frequency filtering with storage of light.

Fig. 1 shows a schematic diagram of the experimental setup. The states  $\{|a\rangle, |b\rangle\}$  and  $|c\rangle$  of a  $\Lambda$  type three level system correspond to  ${}^5\text{S}_{1/2}, F = \{1, 2\}$  and  ${}^5\text{P}_{1/2}, F' = 2$  of the  $^{87}\text{Rb } D_1$  line, respectively. We generated parametric fluorescence by using two independent quasi-phase-matched  $\text{MgO:LiNbO}_3$  waveguides (LN1,2 in Fig. 1) [22, 23]. Optical pulses (pulse width: 190 ns; peak

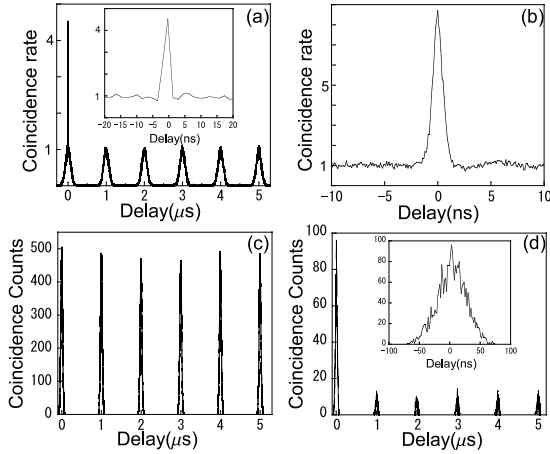


FIG. 2: Experimental results of intensity correlation with 1.6-ns resolution of the MCS: (a) broadband parametric fluorescence, (c) retrieved component of coherent light, and (d) retrieved component of parametric fluorescence. The insets of (a) and (d) show magnifications of the coincidences at 0 time delay. (b) Sharp coincidence peak in (a) measured with 0.1 ns resolution of the MCS.

intensity:  $\sim 110$  mW) were generated by an acousto-optic modulator (AOM1) from the linearly polarized continuous output of a Ti:sapphire laser. The pulses were coupled to LN1 with 50% efficiency and generated second harmonic pulses (pulse width: 130 ns; peak intensity:  $\sim 16$  mW). The second harmonic light was injected into LN2 (coupling efficiency 40%) and the parametric fluorescence was generated. The frequency of the degenerate component in the parametric fluorescence was resonant with the  $|a\rangle \rightarrow |c\rangle$  transition. The frequency bandwidth of the fluorescence was about 10 THz, which was reduced to 23 GHz using a holographic grating (HG) and a polarization maintained single mode fiber (PMF). The output of the PMF was used as broadband probe light. In order to obtain a high extinction ratio between the probe and control lights, the two beams were overlapped at the cold atoms with a crossing angle of  $2.5^\circ$  and an etalon (ET) was inserted into the probe optical axis. The frequency width of the parametric fluorescence was thus reduced to about 600 MHz before detection. The overall transmission efficiency for the degenerate component of the probe light was about 3%.

We first evaluated the intensity correlation function of the obtained broadband probe light. The light was detected by photon counting using silicon avalanche photodiodes (D1, D2; PerkinElmer model SPCM-AQR; detection efficiency: 62%; time resolution: 350 ps). The outputs of D1 and D2 were fed to the start and stop inputs, respectively, of a multi-channel scaler (MCS). Fig. 2(a) shows the normalized coincidence rate as a function of time delay with 1.6 ns resolution. A sharp coincidence peak superposed on a moderate profile of width 0.2  $\mu$ s appears at 0  $\mu$ s, shown magnified in the inset. The moderate profile of the coincidence peak is due to

the shape of the parametric fluorescence pulse. The obtained normalized auto intensity correlation function was  $g^{(2)}(0) = 4.4 \pm 0.2 > 3$  [23], which is called “superbunching”. We remeasured the sharp coincidence peak at 0.1 ns resolution (Fig. 2(b)) to closely evaluate the coherence time of the probe light. The temporal width of the coincidence (full width at half maximum: FWHM) was 1.2 ns with total time resolution 0.8 ns, which means the coherence time of the probe light is about or less than 0.2 ns. The auto intensity correlation function is theoretically given by  $g^{(2)}(0) = 37$  with a squeeze parameter of 0.17 obtained from the classical parametric gain [24], which is much larger than the experimental value. This disagreement can be explained by the longer time resolution (2.3 ns) than the coherence time ( $\leq 0.2$  ns) and fluctuation of the second harmonic light intensity [23]. We note that the superbunching effect is not direct proof of the non-classicality of the light. However, when  $g^{(2)}(0)$  is much greater than 3, the state of the parametric fluorescence can be approximated as a highly bunched photon-pair state i.e.  $|\phi\rangle \approx |0\rangle + \epsilon|2\rangle$  ( $|\epsilon|^2 \ll 1$ ). In our experiment, we prepared the parametric fluorescence such that the fluorescence was in the highly bunched state.

Before performing an experiment with broadband parametric fluorescence, we performed an EIT experiment using narrowband coherent light (spectrum line width  $< 100$  kHz) as probe light. Magneto-optically trapped  $^{87}\text{Rb}$  atoms were used as an optically thick medium, placed in a vacuum cell magnetically shielded by a single permalloy. One cycle of the experiment comprised an atomic medium preparation period (6.3 ms) and a measurement period (3.7 ms). After laser cooling, the magnetic fields and the cooling and repumping lights were turned off, and depumping lights illuminated the atomic ensemble for 45  $\mu$ s, so that all atoms were prepared in state  $|a\rangle$ , where the optical depth of the  $|a\rangle \rightarrow |c\rangle$  transition was  $\sim 6$ . In the measurement period, a weak probe light (beam diameter 330  $\mu$ m) and a 400  $\mu$ W control light (beam diameter 770  $\mu$ m) with the same circular polarizations were injected into the unpolarized atomic ensemble. The control light was generated from a second Ti:sapphire laser and its intensity was varied using an acousto-optic module (AOM2).

Fig. 3 shows probe intensity transmissions as a function of the detuning  $\Delta/2\pi$ , where signals were obtained by sweeping the probe frequency during the measurement period. In the absence of the control light (dotted line), the probe light was absorbed by the atomic medium. With the addition of the control light (solid line), the medium was rendered transparent around  $\Delta/2\pi = 0$  (peak transmission: 77%; FWHM of the transparency window: 8.3 MHz). We classified this EIT spectrum into three regions: (A) transparent, (B) absorption, and (C) off resonant regions. The broadband parametric fluorescence was spread over all regions

We observed the propagation of the coherent probe pulse in the three regions by injecting probe pulses into the cold atoms 3390 times over the measurement period.

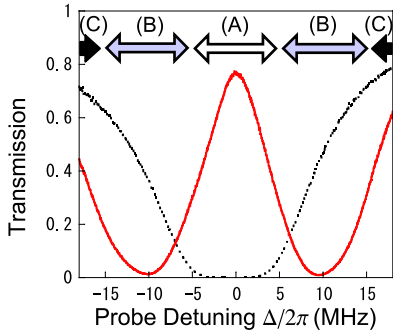


FIG. 3: (Color online) Measured transmission spectra of a weak coherent probe as a function of detuning with (solid line) and without (dotted line) the control light.

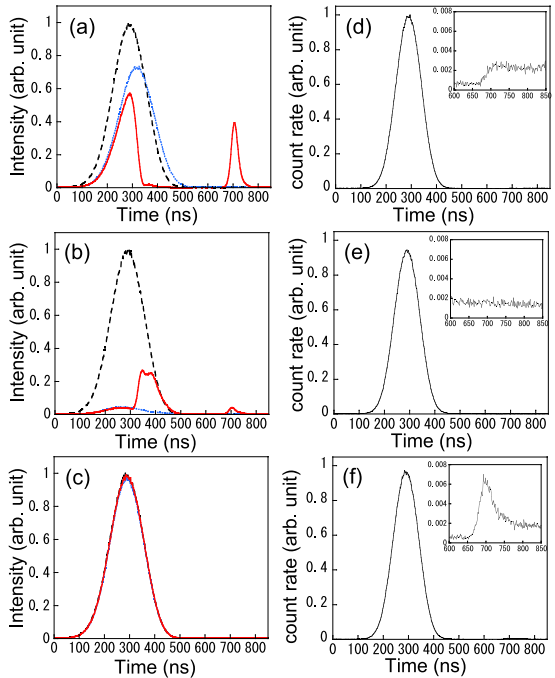


FIG. 4: (Color online) Obtained probe pulses. In the left hand plots, the probe light was coherent light with frequency detuning of (a) 0 MHz, (b) 10 MHz, and (c) 100 MHz under reference (broken line), slow propagation (dotted line), and storage conditions (solid line). See text for details. In the right hand plots, the probe light was broadband parametric fluorescence under (d) reference, (e) slow propagation, and (f) storage conditions. The insets of (d)–(f) show magnifications of the count rate from 600 ns to 850 ns.

Figs. 4(a)–(c) show typical probe signals in the (A)–(C) regions. The broken curves correspond to transmitted probe intensity signals without cold atoms, where the intensity of the control light was dynamically changed (reference condition). The dotted curves correspond to probe signals with cold atoms and constant control light (slow propagation condition). The solid curves show signals with cold atoms and control light with dynamically varied intensity (storage condition). The control light

(intensity:  $400 \mu\text{W}$ ) was turned off from 300 ns to 350 ns and turned on from 650 ns to 700 ns. For probe detuning of  $\Delta/2\pi = 0$  ((A) transparent region), a pulse delay of 25 ns was observed under the slow propagation condition (dotted curve in (a)), which corresponds to more than three orders of magnitude reduction in group velocity. Under the storage condition, the probe pulse was partially stored and retrieved (solid curve). When the probe frequency was detuned by  $\Delta/2\pi = 10 \text{ MHz}$  (absorption (B) region),  $-10 \text{ ns}$  of “superluminal” propagation was observed (dotted curve in (b)), due to anomalous dispersion corresponding to the absorption. Under the storage condition, the probe intensity increased when the control light was tuned off and a slight retrieval was observed when the control light was turned on (solid curve in (b)). The increase of the probe intensity can be explained as being due to a change in the probe transmission from the solid to the dotted curve at  $\Delta/2\pi = 10 \text{ MHz}$  in Fig. 3. The slight retrieval will be due to the frequency component of the probe corresponding to the transparent (A) region, since the frequency width of a light pulse is given by the inverse of its temporal width. When the probe was detuned by  $\Delta/2\pi = 100 \text{ MHz}$ , the probe signals were almost identical under each of the conditions (Fig. 4(c)). Fig. 2(c) shows the intensity correlation of the retrieved component in Fig. 4(a), where the outputs of D1 and D2 were gated from 675 ns to 745 ns. The obtained intensity correlation function  $g^{(2)}(0) = 1.05 \pm 0.01$  agrees with that of coherent light ( $g^{(2)}(0) = 1$ ) [25].

Finally, we observed the propagation of broadband parametric fluorescence under EIT. Figs. 4(d)–(f) show photon count rates as a function of time under reference, slow propagation, and storage conditions, respectively. The insets show magnifications of the count rates from 600 ns to 850 ns. The experimental conditions were the same as for the case of the probe light in the coherent state. Since the frequency width of the probe light was broad, corresponding phenomena from each of the regions occurred simultaneously. There was almost no difference between (d) and (e), since the dominant frequency components of the probe were far from resonance. However, (f) was slightly different from (d) and (e). There was a small retrieved component from 650 ns to 750 ns. The insets of (d) and (e) show residual control light under reference and slow propagation conditions, respectively. The inset of (f) shows the clear retrieved component. The height of the retrieved component was 0.007 of that of the injected probe light, which agrees with the product of the reduction of the frequency width ( $8.3 \text{ MHz}/600 \text{ MHz}$ ) and retrieval efficiency (40%) in (a).

Fig. 2(d) shows the intensity correlation of the retrieved component. The obtained normalized auto intensity correlation function was  $g^{(2)}(0) = 9.0 \pm 0.2 > 3$ , i.e. superbunching was obtained, where the coincidence count rate was  $0.4 \text{ s}^{-1}$ . The coincidence at 0 time delay in Fig. 2 (a) has a sharp peak superposed on a moderate profile, while that in (d) does not have such a double structure, where the signals were obtained under the

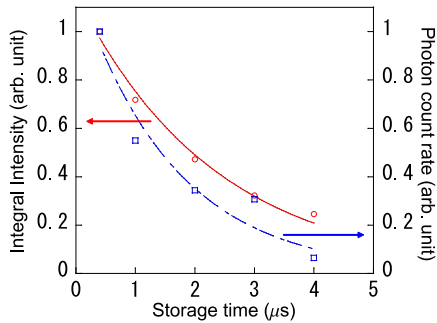


FIG. 5: (Color online) Integral intensities of retrieved coherent lights and photon count rates of retrieved parametric fluorescence as a function of storage time.

same time resolution. The observed coherence time of the retrieved light was  $\sim 35$  ns, which is much longer than that of the incident probe pulse. The increase of the coherence time shows that frequency filtered storage and retrieval occurred, that is, we have demonstrated the time-frequency filtering with storage of light technique. The experimentally obtained  $g^{(2)}(0)$  should be equal to the theoretical value of 37, since the coherence time was larger than the time resolution for detection. The disagreement can be explained by the mixing of residual control light (coherent light  $g^{(2)}(0) = 1$ ) and the storage of temporally non-correlated photons caused by fluctuation of the center frequency of the probe light relative to the center of the EIT window.

Fig. 5 shows the integral intensities of the retrieved coherent light and photon count rates of the retrieved parametric fluorescence (the offset due to the residual

control light was subtracted) as a function of storage time. The obtained  $1/e$  decay times were  $2.3 \mu\text{s}$  and  $1.6 \mu\text{s}$  for coherent light and parametric fluorescence, respectively. Signal decay was the result of the destruction of atomic coherence, which was in our experiment caused by residual magnetic fields due to eddy currents. The small difference in the atomic coherence times may be caused by a disturbance of the collective atomic state due to absorptions of the broadband parametric fluorescence in the absorption (B) region .

In conclusion, we have demonstrated frequency filtered storage of broadband parametric fluorescence (highly bunched photon-pair state). The frequency component of the fluorescence within an electromagnetically induced transparency window was stored in an atomic ensemble and then retrieved after other components had passed through the atoms, confirmed by the observation of superbunching and from evaluating the coherence time for the retrieved light. This experiment also demonstrated the time-frequency filtering with storage of light technique. While the observation of the superbunching effect is not direct proof of the nonclassicality of the light, the results obtained here are the first steps toward the generation of various nonclassical states of atomic ensembles with the widely used parametric down conversion process.

We gratefully acknowledge R. Inoue, D. Akamatsu and Y. Yokoi. One of the authors (K. A.) was partially supported by the JSPS. This work was supported by a Grant-in-Aid for Scientific Research (B) and the 21st Century COE Program at Tokyo Tech “Nanometer-Scale Quantum Physics” by MEXT.

---

[1] M. Fleischhauer and M. D. Lukin, *Phys. Rev. Lett.* **84**, 5094 (2000).  
[2] M. Fleischhauer and M. D. Lukin, *Phys. Rev. A* **65**, 022314 (2002).  
[3] S. E. Harris, *Phys. Today* **50** (7), 36 (1997).  
[4] T. Chanelière *et al*, *Nature (London)* **438**, 833 (2005).  
[5] M. D. Eisaman *et al*, *Nature (London)* **438**, 837 (2005).  
[6] D. N. Matsukevich *et al*, *Phys. Rev. Lett.* **96**, 030405 (2006).  
[7] L.-A. Wu *et al*, *Phys. Rev. Lett.* **57**, 2520 (1986).  
[8] L. Mandel, *Rev. Mod. Phys.* **71**, S274 (1999).  
[9] P. G. Kwiat *et al*, *Phys. Rev. Lett.* **75**, 4337 (1995).  
[10] D. Bouwmeester *et al*, *Nature (London)* **390**, 575 (1997).  
[11] N. Gisin *et al*, *Rev. Mod. Phys.* **74**, 145 (2002).  
[12] M. Koashi, M. Matsuoka, and T. Hirano, *Phys. Rev. A* **53**, 3621 (1990).  
[13] Y. J. Liu and Z. Y. Ou, *Phys. Rev. Lett.* **88**, 023601 (2002).  
[14] J. T. Barreiro *et al*, *Phys. Rev. Lett.* **95**, 260501 (2005).  
[15] D. Bouwmeester *et al*, *Phys. Rev. Lett.* **82**, 1345 (1999).  
[16] M. Eibl *et al*, *Phys. Rev. Lett.* **92**, 077901 (2004).  
[17] P. Walther *et al*, *Nature (London)* **434**, 169 (2005).  
[18] D. Akamatsu and M. Kozuma, *Phys. Rev. A* **67**, 023803 (2003).  
[19] A. K. Patnaik, F. L. Kien, and K. Hakuta, *Phys. Rev. A* **69**, 013819 (2004).  
[20] C. Liu *et al*, *Nature (London)* **409**, 490 (2001).  
[21] R. N. Shakhmuratov and J. Odeurs, *Phys. Rev. A* **71**, 013819 (2005).  
[22] D. Akamatsu, K. Akiba, and M. Kozuma, *Phys. Rev. Lett.* **92**, 203602 (2004).  
[23] K. Akiba, D. Akamatsu, and M. Kozuma, *Opt. Commun.* **259**, 789 (2006).  
[24] R. Loudon, *The Quantum Theory of Light* (Oxford University Press, New York, 2000), 3rd ed.  
[25] The intensity correlation function of the retrieved component in Fig. 4(b) was measured to be  $g^{(2)}(0) = 1.06 \pm 0.01$ .